Journal of Alloys and Compounds 699 (2017) 517–520

Contents lists available at ScienceDirect

Journal of Alloys and Compounds

journal homepage: http://www.elsevier.com/locate/jalcom

Synthesis of Cu_2SnS_3 nanosheets as an anode material for sodium ion batteries

Liang Shi [a, *], Wenhui Wang [b], Chunyan Wu [a], Jia Ding [a], Quan Li [b]

[a] Department of Chemistry, University of Science and Technology of China, Hefei 230026, PR China
[b] Department of Physics, The Chinese University of Hong Kong, Shatin, New Territory, Hong Kong, China

ARTICLE INFO

Article history:
Received 8 October 2016
Received in revised form
31 December 2016
Accepted 2 January 2017
Available online 3 January 2017

Keywords:
Nanostructured materials
Electrode materials
Cu_2SnS_3
Chemical synthesis
Transmission electron microscopy

ABSTRACT

Single crystalline Cu_2SnS_3 nanosheets with exposed (220) planes have been synthesized via a facial solvothermal solution chemical route. The solvent of ethylenediamine hindered the growth along the [110] direction and facilitated the formation of two dimensional nanostructures. Electrochemical performance of Cu_2SnS_3 electrodes in sodium ion batteries was investigated. Cu_2SnS_3 electrodes exhibit an initial sodiation capacity of 586 mAh/g and 178 mAh/g after 50 cycles. The electrochemical properties of Cu_2SnS_3 nanosheets suggest it is a potential anode material for sodium ion batteries.

1. Introduction

Cu_2SnS_3 is an important I-V-VI ternary chalcogenide semiconductor and has attracted increasing attention in recent years. Cu_2SnS_3 has various unique properties including high absorption coefficients, an optimal band gap (about 1 eV), a carrier concentration of 1.85×10^{20} cm^{-3} and a Hall mobility of 1.79 cm^2 V^{-1} s^{-1} [1–3]. These properties offer Cu_2SnS_3 potential applications in many fields, such as thin film waveguides, light emitting diodes, nonlinear optics, photocatalysis. Cu_2SnS_3 has also a special advantage due to its containing naturally abundant elements Cu, Sn and S, as well as its non-toxicity. In addition, Cu_2SnS_3 exhibits good conducting ability and there are interlayer spaces and tunnels in its crystal structure, which make it to be an ideal lithium-ion electrode material [4]. Mesoporous Cu_2SnS_3 spheres have been synthesized and electrochemical tests indicated that this structure could promote the transfer of electrolyte and lithium ions, resulting in great enhancement of the cycling performances [5]. Cu_2SnS_3 cabbage-like nanostructures were found to show electrochemical performance of lithium ion anodes with highly reversible capacity and excellent stability [6]. Cu_2SnS_3 flowers, Cu_2SnS_3 hollow microspheres and Cu_2SnS_3/reduced graphene oxide composites have also been reported to be utilized as active electrode materials in lithium ion batteries and give evidence that the unique crystal structure of Cu_2SnS_3 facilitated the insertion/extraction of lithium ion during the electrochemical process in Cu_2SnS_3/Li cells [7–10].

On the other hand, though lithium-ion batteries have been well developed as rechargeable energy storage for electric vehicles and portable electronics, the high cost and limited Li-containing mineral resources make it an important issue the sustainable and wide range of business applications of lithium-ion batteries [11,12]. As a potential alternative to lithium-ion batteries, sodium-ion batteries have recently gained much attention because of their similarities to lithium-ion batteries and low cost, abundant availability of Na resources [13–15]. As for Cu_2SnS_3, interlayer distance of2.280 Å and the tunnel size of $3.921\times5.587\times4.210$ $Å^3$ in its supercell crystal structure are lager than the diameter of sodium ion (radius 0.95 Å). Therefore, sodium ion diffusion through the Cu_2SnS_3 crystal structure should be possible, which makes Cu_2SnS_3 a potential ideal anode material in sodium-ion batteries. However, to the best of our knowledge, there has no report that Cu_2SnS_3 is employed as an active sodium ion electrode material. Here, we report a solution chemical route to synthesize Cu_2SnS_3 nanosheets with exposed planes of (220). The as prepared Cu_2SnS_3 nanosheets have been investigated as a novel electrode material for sodium ion batteries in half-cells. Our research indicated that Cu_2SnS_3 offers a new

* Corresponding author.
E-mail address: sliang@ustc.edu.cn (L. Shi).

http://dx.doi.org/10.1016/j.jallcom.2017.01.023
0925-8388/

alternative to anode materials in Na cells.

2. Experimental section

2.1. Synthesis

All reagents are analytical grade and used without further purification. In a typical procedure for the preparation of Cu_2SnS_3 nanosheets, 3 mmol sulfur powder, 2 mmol $CuCl_2 \cdot 2H_2O$, 1 mmol $SnCl_4 \cdot 5H_2O$, and 18 mL anhydrous ethylenediamine (En) were added to a 50 mL beaker in air. The mixture was treated with mild magnetic stirring for 5 min before being transferred into a 20 mL stainless steel teflon-lined autoclave. The autoclave was sealed and the temperature was maintained at 220 °C for 24 h before being cooled down to room temperature. The precipitate was separated by centrifugation, washed with distilled water and absolute ethanol several times, and finally dried in vacuum at 40 °C for 4 h.

2.2. Material characterization

The overall crystallinity of the product is examined by X-ray diffraction (XRD, Rigakau RU-300 with CuKα radiation). The general morphology of the products was characterized using scanning electron microscopy (FESEM QF400). Detailed microstructure analysis was carried using transmission electron microscopy (TEM Tecnai 20ST).

2.3. Electrochemical measurements

The electrochemical measurements were carried out by assembly of 2032 coin cells in a glove box filled with pure argon gas, using Na foil as both the counter electrode and reference electrode. 1 M NaClO4 dissolved in propylene carbonate (PC) with 5 wt% fluoroethylene carbonate (FEC) additive as electrolyte, and a GD-120 glass fiber filter as separator. The working electrodes were prepared by mixing the as-synthesized materials, acetylene black, and carboxyl methyl cellulose sodium salt (NaCMC) at the weight ratio of 60:20:20. The slurry was casted onto Cu foil and dried in a vacuum oven at 60 °C overnight. The mass loading of active materials was about 1.2 mg. Galvanostatic charge-discharge tests were performed at a potential range of 0.01–3 V *vs.* Na/Na^+ using a multichannel battery testing system (LAND CT2001A). Cyclic voltammetry (CV) was tested with an electrochemical workstation (CHI6009D).

3. Results and discussion

The crystal structure of the product was characterized by X-ray diffraction (XRD) to obtain information on crystal structure and phase composition. The product is phase-pure Cu_2SnS_3 as determined. A typical XRD pattern of the Cu_2SnS_3 product is shown in Fig. 1, which can be indexed to be face-centered cubic structure. The refined lattice constants of the Cu_2SnS_3 are $a = 5.41$ Å, according with the reported value for Cu_2SnS_3 crystal (JCPDS card, No. 89-2877). The broadening peaks in the XRD pattern suggest that the grain size of the Cu_2SnS_3 product is on a nanometer scale. It is found that the relative intensity of the (220) peak is stronger than that in the JCPDS file, suggesting preferential orientation of the Cu_2SnS_3 nanostructure normal to the [110] direction, as is further demonstrated by the TEM analysis in later section.

The SEM image in Fig. 2 (a) shows an overview of the as-prepared Cu_2SnS_3 products. It is apparent the product consists of a large quantity of sheets with size of 1–2 μm. Some nearly vertically nanosheets discloses that these sheets have thickness of about 50–70 nm. A typical TEM image of Cu_2SnS_3 nanosheets in Fig. 2 (b)

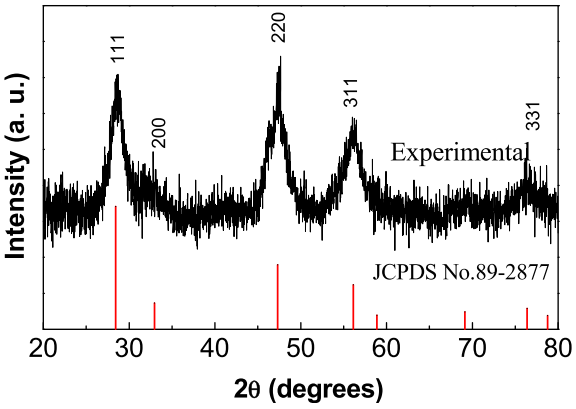

Fig. 1. A representative XRD pattern of Cu_2SnS_3 nanosheets.

shows they are almost semi-transparent under TEM electron beam due to very thin thickness. The lower left inset of Fig. 2 (b) is a selected area electron diffraction (SAED) pattern of a nanosheets, showing clearly sing crystalline symmetrical diffraction spots. The SAED patten can be indexed to the [110] zone of the cubic structured Cu_2SnS_3. The electron beam was most likely aligned perpendicular to the flat surface, therefore, it can be concluded that the flat surfaces of the sheets are perpendicular to the [110] direction. That is to say, exposed planes of the Cu_2SnS_3 nanosheets are (220) planes. This is consistent with the XRD result in Fig. 1, in which the relative intensity of the (220) peak in the XRD pattern of the nanosheets become much stronger comparing with that of JCPDS No. 89-2877. A HRTEM image of the Cu_2SnS_3 nanosheets in the upper right inset of Fig. 2 (b) displays a clear lattice spacing of 0.31 nm corresponding to the d spacing of the (111) planes in cubic structured Cu_2SnS_3, confirming further the highly crystalline nature of the as prepared nanosheets.

Ethylenediamine acted as a solvent in the reaction and played an important role in the preparation of Cu_2SnS_3 nanostructures with a nanosheets shape. If we used distilled water, instead of ethylenediamine, as a solvent in the experiment with other reaction conditions unchanged, Cu_2SnS_3 nanoparticles with an irregular shape can be obtained.

Fig. 3a shows a typical XRD pattern of Cu_2SnS3 nanoparticles prepared with a distilled water solvent. All diffraction peaks can be indexed to face-centered cubic structured Cu_2SnS_3. The obviously broadening of XRD peaks suggests that the as-prepared Cu_2SnS_3 particles are of very small sizes. Based on the Scherrer equation, $D=(0.89\lambda)/\beta(\cos\theta)$, here λ is the wavelength for the Cu $K\alpha_1$ (1.54056 Å) radiation, β is the peak width at half-maximum in radians and θ is the Bragg's angle, the average particle size was calculated to be 110 nm. The particle size result is consistent with later TEM analysis. A TEM image in Fig. 3b indicates that the as-prepared product is composed of a lot of aggregated nanoparticles with size in the range of 100–150 nm. The diffraction rings of the selected area electron diffraction (SAED) pattern taken from these nanoparticles, as displayed in the inset of Fig. 3b, reveal polycrystalline nature of Cu_2SnS_3 sample and can be indexed to (111), (220) and (311) reflections, consistent with the expected cubic crystal lattice.

The above results indicate that ethylenediamine solvent is necessary in the formation of two dimensional Cu_2SnS_3 nanosheets. In our present solution approach, we believe that ethylenediamine acts as both a chelating agent and a surface-passivating agent. Ethylenediamine has been known to be a strong chelating agent. Ethylenediamine chelated with metal ions of Cu^+ and Sn^{4+} and formed complex ions. This will level much and balance the

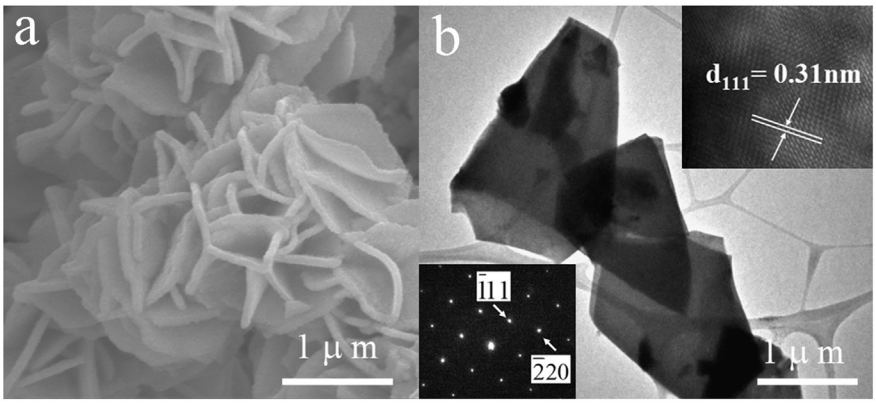

Fig. 2. SEM image (a) and TEM image (b) of the as-prepared Cu_2SnS_3 nanosheets; The lower left inset of Fig. 2 (b) shows a selected area electron diffraction pattern and the upper right inset of Fig. 2 (b) shows a HRTEM (c) image.

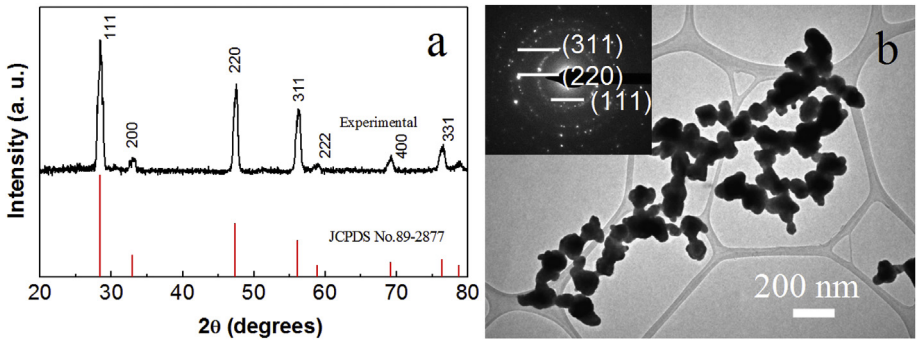

Fig. 3. XRD pattern (a), TEM image (b) and the corresponding SAED pattern (inset of b) of the as-prepared polycrystalline Cu_2SnS_3 nanoparticles obtained from the reaction by using distilled water instead of ethylenediamine as the solvent.

reactivity difference of the cationic precursors, avoiding the formation of binary sulfides. As a result, pure phase ternary Cu_2SnS_3 nanocrystals become favorable generated [16]. Meanwhile, ethylenediamine is a good solvent of element sulfur. The sulfur powder was dissolved in ethylenediamine with stirring, evidenced by the change of the solution color from opaque to yellow and the disappearance of the sulfur powder. Ethylenediamine then reduced the dissolved elemental S to negatively charged S^{2-} with an organic nucleophilic attack. S^{2-} reacted with the En chelated Cu^{+}, Sn^{4+} complex to form Cu_2SnS_3 molecules. After the nucleation of Cu_2SnS_3 molecules, grain growth begins. Here, we believe that, the ethylenediamine molecules can control the growth rates of different crystalline facets of Cu_2SnS_3 by interacting with these facets through selective absorption and desorption. It can be presumed that the wide exposed (220) planes of Cu_2SnS_3 nanosheets are completely passivated by ethylenediamine while the side normal planes are partially passivated. Therefore the ethylenediamine absorbs or binds strongly on the (220) planes, hinder the growth along the [110] direction. So, the two dimensional Cu_2SnS_3 nanosheet shape was formed finally after long time crystal growth.

Fig. 4 shows the charge–discharge profiles (cycles 1, 2, 5, 10 and 50) of the Cu_2SnS_3 nanosheets electrode vs. Na half-cell at a current density of 30 mA/g and in the voltage range from 0 to 2.5 V. During the first discharge (sodiation) process, two potential plateaus at about 1.3 V and 0.75 V appeared. However, the plateau at 1.3 V disappeared in the subsequent discharge curves, suggesting an irreversible reaction may occur at this potential. In the first charge (de-sodiation) process, a plateau at about 1.55 V and a slope between 2.05 and 2.15 V can be observed. It is found that the initial

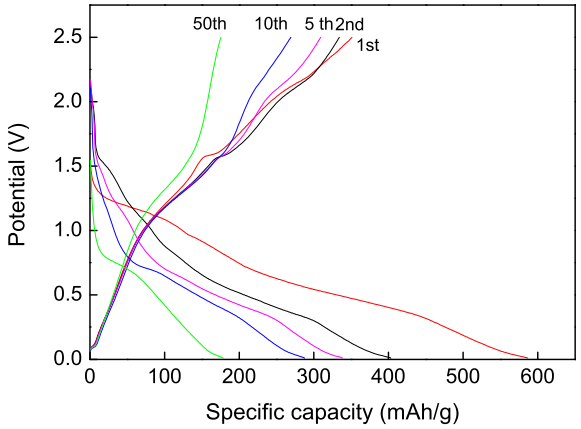

Fig. 4. The charge and discharge curves of the Cu_2SnS_3 nanostructures at a current density of 30 mA/g.

discharge and charge capacities are 586 and 351 mAh/g, with an initial coulombic efficiency of 59.5%. The initial capacity loss should originate from the formation of a solid electrolyte interface (SEI) or incomplete conversion reaction. The coulombic efficiency increased rapidly to nearly 100% and then kept stable, as the values of coulombic efficiency for 2nd, 5th, 10th and 50th cycle are 82.9%, 91.4%, 93.7%, 98.3%, respectively.

The cycling performance of Cu_2SnS_3 nanosheets electrode vs. Na half-cell between 0 and 2.5 V at a current density of 30 mA g^{-1} is showed in Fig. 5. After 50 cycles, the discharge capacity of Cu_2SnS_3

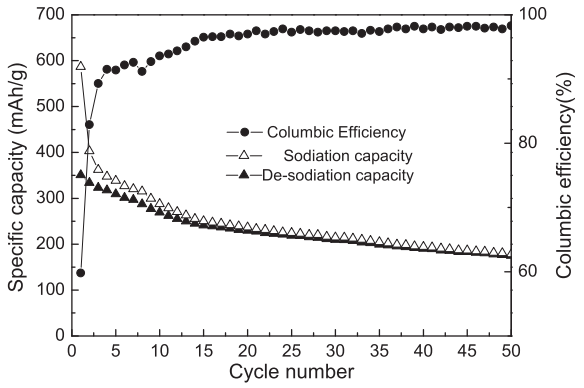

Fig. 5. Cycling behaviour of Cu_2SnS_3 nanosheets electrode at a current density of 30 mA/g.

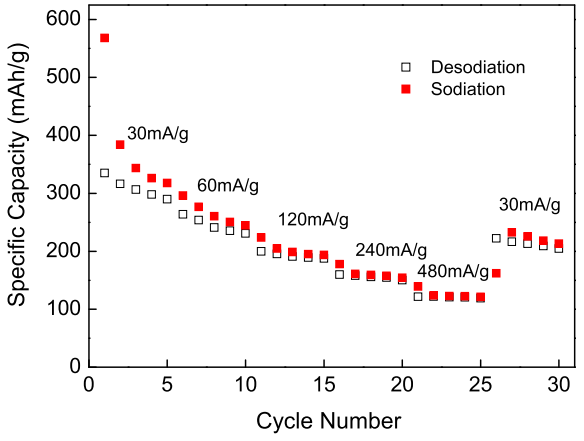

Fig. 6. Rate performance of Cu_2SnS_3 nanosheets electrode.

nanosheets electrode descended from 586 mAh/g to 178 mAh/g.

The rate performance of Cu_2SnS_3 nanosheets electrode was evaluated at different charge–discharge current rates in the voltage range 0–2.5 V, as shown in Fig. 6. At each rate, the storage capacity is stable except at a low rate of 30 mA/g. The electrode delivers reversible capacities of 335, 264, 199, 160 and 121 mAh/g at a charge–discharge current of 30, 60, 120, 240 and 480 mA/g, respectively. As expectedly, the capacity decreased gradually with increasing rate, possibly induced by a diffusion-limited mass transfer of Na^+ between the surface and core of the Cu_2SnS_3 nanosheets. After the current density returns to 30 mA/g, a capacity of 222 mAh/g was obtained.

4. Conclusions

In conclusion, single-crystalline Cu_2SnS_3 nanosheets with thickness in the range of about 50–70 nm have been synthesized through a simple solvothermal solution strategy. The as-prepared Cu_2SnS_3 nanosheets are face-centered cubic structured and oriented parallel to the (220) crystal plane. Ethylenediamine exerted a strong surface-passivating effect on (220) crystal planes of Cu_2SnS_3 and led to the final shape of nanosheets. Electrochemical tests show Cu_2SnS_3 is a potential electrode material for sodium ion batteries.

Acknowledgements

This work was supported by the National Natural Science Foundation of China (No. 21371163).

References

[1] X.Y. Chen, X. Wang, C.H. An, J.W. Liu, Y.T. Qian, J. Cryst. Growth 256 (2003) 368–376.
[2] B. Li, Y. Xie, J.X. Huang, Y.T. Qian, J. Sol. Stat. Chem. 153 (2000) 170–173.
[3] G. Marcano, C. Rincon, G. Marin, R. Tovar, G. Delgado, J. Appl. Phys. 92 (2002) 1811–1815.
[4] C.Z. Wu, Z.P. Hu, C.L. Wang, H. Sheng, J.L. Yang, Y. Xie, Appl. Phys. Lett. 91 (2007) 143104–143106.
[5] B.H. Qu, M. Zhang, D.N. Lei, Y.P. Zeng, Y.J. Chen, L.B. Chen, Q.H. Li, Y.G. Wang, T.H. Wang, Nanoscale 3 (2011) 3646–3651.
[6] B. Qu, H. Li, M. Zhang, L. Mei, L. Chen, Y. Wang, Q. Li, T. Wang, Nanoscale 3 (2011) 4389–4393.
[7] X.J. Liang, Q. Cai, W.D. Xiang, Z.P. Chen, J.S. Zhong, Y. Wang, M.G. Shao, Z.R. Li, J. Mater. Sci. Technol. 29 (2013) 231–236.
[8] H.C. Tao, S.C. Zhu, X.L. Yang, L.L. Zhang, S.B. Ni, J. Electroanal. Chem. 760 (2016) 127–134.
[9] Z.A. Zhang, Y. Fu, C.K. Zhou, J. Li, Y.Q. Lai, Solid. State. Ionics 269 (2015) 62–66.
[10] Z. Zhang, C. Zhou, M. Jia, Y. Fu, J. Li, Y. Lai, Electrochim. Acta 143 (2014) 305–311.
[11] W. Luo, M. Allen, V. Raju, X. Ji, Adv. Energy. Mater. 4 (2014) 1400554.
[12] J.M. Tarascon, Nat. Chem. 2 (2010) 510.
[13] V. Palomares, P. Serras, I. Villaluenga, K.B. Hueso, J. Carretero-Gonzalez, T. Rojo, Energy Environ. Sci. 5 (2012) 5884–5901.
[14] D. Kim, S.H. Kang, M. Slater, S. Rood, J.T. Vaughey, N. Karan, M. Balasubramanian, C.S. Johnson, Adv. Energy. Mater. 1 (2011) 333–336.
[15] M.D. Slater, D. Kim, E. Lee, C.S. Johanson, Adv. Funct. Mater. 23 (2013) 947–958.
[16] R.G. Xie, M. Rutherford, X.G. Peng, J. Am. Chem. Soc. 131 (2009) 5691–5697.